Human Molecular Genetics, 2005, Vol. 14, No. 22 ***3477–3492***
doi:10.1093/hmg/ddi377
Advance Access published on October 5, 2005

Mitochondrial import and enzymatic activity of PINK1 mutants associated to recessive parkinsonism

Laura Silvestri[1,†], Viviana Caputo[2,3,†], Emanuele Bellacchio[2], Luigia Atorino[1], Bruno Dallapiccola[2,3], Enza Maria Valente[2] and Giorgio Casari[1,4,*]

[1]Human Molecular Genetics Unit, Dibit-San Raffaele Scientific Institute, Milan, [2]IRCCS CSS, Mendel Institute, Rome, [3]Department of Experimental Medicine and Pathology, La Sapienza University, Rome and [4]Vita-Salute San Raffaele University, Milan, Italy

Received August 18, 2005; Revised and Accepted September 29, 2005

Parkinson's disease (PD) is a progressive neurodegenerative illness associated with a selective loss of dopaminergic neurons in the nigrostriatal pathway of the brain. Despite the overall rarity of the familial forms of PD, the identification of single genes linked to the disease has yielded crucial insights into possible mechanisms of neurodegeneration. Recently, a putative mitochondrial kinase, PINK1, has been found mutated in an inherited form of parkinsonism. Here, we describe that PINK1 mutations confer different autophosphorylation activity, which is regulated by the C-terminal portion of the protein. We also demonstrate the mitochondrial localization of both wild-type and mutant PINK1 proteins unequivocally and prove that a short N-terminal part of PINK1 is sufficient for its mitochondrial targeting.

INTRODUCTION

Parkinson's disease (PD) is a frequent neurodegenerative disorder with age-related prevalence close to 2% in the seventh decade of life. The core clinical features of resting tremor, rigidity and bradykinesia are caused by a severe degeneration of dopaminergic neurons of the substantia nigra.

Although most PD cases are sporadic, dominant mutations in α-synuclein and LRRK2/dardarin and recessive mutations in parkin and DJ-1 have been linked to familial forms of parkinsonisms, which resemble idiopathic PD.

The characterization of Mendelian causes of PD has provided tremendous insights into the pathogenesis of this disorder, unraveling complex pathogenetic mechanisms in which mitochondrial dysfunction, protein misfolding and impairment of the ubiquitin-proteasome system concur to the neurodegenerative process (1,2). However, the precise pathways underlying dopaminergic dysfunction and degeneration are still largely unclear.

Recently, we identified a third gene, PTEN-induced kinase 1 (PINK1), causing autosomal recessive parkinsonism (3). Several nonsense and missense PINK1 mutations have been reported, with a broad phenotypic spectrum ranging from early onset parkinsonism with atypical features to clinical presentations indistinguishable from sporadic late onset PD (4–6).

The PINK1 gene comprises eight exons and codes for a 581 amino acids protein that is ubiquitously expressed; higher level of expression was observed in heart, skeletal muscle and testis (7). Primary sequence prediction analysis of the 63 kDa PINK1 protein identified an N-terminal mitochondrial signal and a catalytic serine–threonine kinase domain (3). Autophosphorylation data supported the kinase potential of PINK1 protein (8).

The identification of PINK1 as a putative mitochondrial protein kinase upholds previous reports, showing that abnormal phosphorylation and mitochondrial dysfunction play major roles in PD pathogenesis (9). It has been recently

*To whom correspondence should be addressed at: Human Molecular Genetics Unit, San Raffaele Scientific University Institute, DIBIT, Via Olgettina 58, 20132 Milan, Italy. Tel: +39 0226433502/4721/4947; Fax: +39 0226434767; Email: casari.giorgio@hsr.it
†These authors contributed equally.

shown that parkin is constitutively phosphorylated and that this post-translational modification is modulated by some cellular stresses, such as proteasomal dysfunction and endoplasmic reticulum stress (10). Abnormal, extensive phosphorylation at serine residue 129 of α-synuclein is typically found in synucleinopathy lesions such as Lewy bodies and Lewy neurites, and it is thought to increase α-synuclein neurotoxicity and propensity to aggregate into abnormal oligomeric species, as it has been recently demonstrated in a *Drosophila* model of PD (11,12). Recently, an additional protein kinase, LRRK2/dardarin, has been found mutated in a dominant form of PD (13,14).

A growing body of evidence suggests that mitochondrial dysfunction could represent the first event triggering neurodegeneration (15). It is known that methyl-4-phenyl-1,2,3,6-tetrahydropyridine (MPTP), a synthetic drug causing a PD-like phenotype, and the pesticide rotenone lead to neuronal cell death by inhibiting complex I activity, thus blocking the mitochondrial respiratory chain (1,16). Reduced complex I activity and markers of oxidative stress have been detected in brains of patients with sporadic PD (17) and both *in vitro* and *in vivo* studies have demonstrated a bi-directional link between mitochondrial impairment, oxidative stress and increased α-synuclein aggregation (18–21). In response to oxidative stimuli, DJ-1 is converted into a more acidic variant and is relocated to the mitochondria, where it exerts its function protecting neurons from death (22). Still, PINK1 is the first protein directly linking mitochondrial abnormalities to a PD phenotype.

Here, we describe the unequivocal localization of PINK1 to the mitochondria and characterize its biochemical properties and catalytic activity of wild-type and mutants PINK1 isoforms. Also, our data show the presence of a carboxy-terminus domain regulating autophosphorylation activity and suggest a decreased autophosphorylation potential of PINK1 mutants, hence functionally linking PARK6 mutations to this mitochondrial kinase.

RESULTS

PINK1 functional domain organization

Analysis of the 581 amino acid primary sequence of PINK1 revealed the presence of a putative mitochondrial leader peptide (LP) at the N-terminus with two possible cleavage sites at amino acids 35 and 77 [MitoProt (23) and TargetP, respectively], a possible transmembrane domain [amino acids 101–107; DAS Transmembrane Prediction (24)] and a serine–threonine kinase domain (amino acids 156–509). Different subdomains can be identified within the kinase domain, according to the classification of Hanks and Hunter (Fig. 1). In particular, subdomains I–IV represent the N-terminal lobe that is involved in anchoring and orienting the ATP molecule, whereas subdomains VIa–XI represent the C-terminal lobe in charge of the binding of the peptide substrate and of phospho-transfer.

Several PINK1 mutations have been reported so far. We concentrated on two missense and one nonsense mutations. Alanine 168 to proline replacement (A168P) affects the highly conserved ATP binding region (subdomain I), whereas the neutral amino acid glycine 309 is substituted by negatively charged aspartic acid (G309D). The nonsense W437X mutation truncates the protein at position 436 and, when transfected in mammalian cells, produces a stable protein of about 48 kDa (see following sections).

Protein modeling

The A168P mutation introduces a proline residue, which is known to be an α-helix- and β-sheet breaker. This can be critical for PINK1, because the alanine 168 is part of the nucleotide phosphate-binding region, which is characterized by local beta-sheet conformations, as determined by structural analysis of homologous proteins. As this region contributes to the ATP/ADP binding necessary for kinase activity, we have further examined the implications of the A168P mutation on the protein structure and/or function. For this purpose, we have carried out molecular dynamics (MD) studies on PINK1 wild-type and PINK1^{A168P} mutant. Interestingly, the MD simulations of the wild-type and of the PINK1^{A168P} mutant show significant differences of protein motion around this region. In the wild-type protein, only moderate amino acid fluctuations are observed and the volume of the protein pocket near the nucleotide phosphate-binding region is kept constant for the whole duration of the MD. Conversely, owing to alteration of the hydrogen bond patterns introduced by the PINK1^{A168P} mutation, irregular fluctuations cause the nucleotide phosphate-binding region to behave like a loose lid and larger variations can be observed in the volume of the associated protein pocket. The volume of the pocket for PINK1 and PINK1^{A168P} mutants at different simulation times is shown in Figure 2A. Figure 2B shows the structures of the wild-type (upper panel) and of the PINK1^{A168P} mutants (lower panel) obtained after 50 ps of MD simulation. These results highlight a predicted structural alteration in the protein region surrounding the nucleotide phosphate-binding region that can alter the interaction between Pink1 and its natural substrates as well as different kinetics of ATP/ADP binding.

In Figure 2C, the glycine 309 and lysine 186 residues are shown as pink and yellow spheres. This latter is predicted to be the catalytic residue implicated in the phosphate group transfer from ATP to protein substrates. Considering that in the PINK1^{G309D} mutant a negatively charged residue replaces a neutral residue in proximity of the catalytic lysine, a phosphomimetic residue is generated near the catalytic site. Potential implications of this mutation are either alteration of substrate recognition or interference with the kinetics of the phosphoryl group transfer.

The residues necessary for kinase activity in PINK1 are maintained in the PINK1^{W437X} mutant. This implies that the truncated protein potentially conserves its phosphorylation activity. By observing the PINK1/substrate model (Fig. 2D), it can be noted that the protein portion missing in PINK1^{W437X} (evidenced in purple) has several residues in contact with the substrate (represented as green sticks). In the proposed model, the lack of the C-terminal part would lead to decreased steric hindrance near the catalytic site with the potential implication of increased probability of substrate access to the active site, hence increasing the propensity of the truncated protein toward non-specific protein phosphorylation.

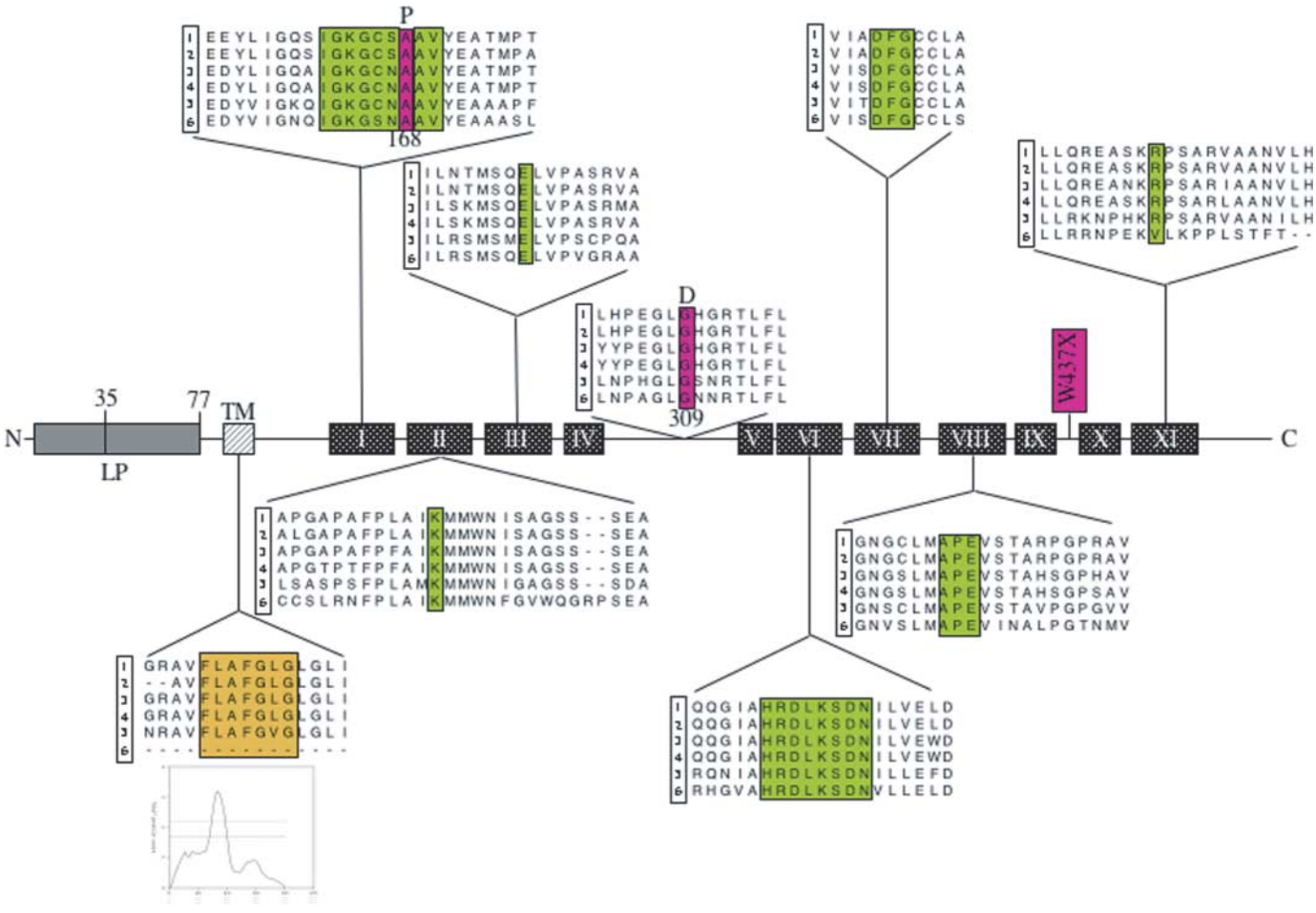

Figure 1. Schematic representation of PINK1 domain structure. Serine–threonine kinase conserved residues are green-boxed. PINK1 substitution or missing portion is boxed in purple. Subdomain I includes residues anchoring ATP moiety. Subdomain II contains the invariant lysine that helps orienting ATP, and forms a salt bridge with the –COOH of glutamic acid (subdomain III). Subdomain VI is characterized by the presence of the catalytic loop HRDLKxxN. Subdomain VII contains the highly conserved DFG motif that chelates Mg^{2+} ions and orients the γ-phosphate of ATP. Subdomain VIII harbors the APE motif, which forms an ion pair with the invariant arginine in subdomain XI, thereby stabilizing the large lobe. Subdomains IV and V are structurally important, whereas subdomains IX and X stabilize the domains and are involved in substrate recognition. Sequence alignment as follows: 1, *Homo sapiens*; 2, *Macaca fascicularis*; 3, *Rattus norvegicus*; 4, *Mus musculus*; 5, *Danio rerio*; 6, *Tetraodon nigroviridis*. TM, possible transmembrane domain; the inset shows TM hydrophobicity [DAS (24)].

Intracellular localization of wild-type and mutant PINK1 proteins

We previously reported the generation of an expression PINK1 plasmid with a c-Myc tag inserted upstream the LP at the N-terminus of the protein (4). However, to avoid interference with the physiological mitochondrial import mechanisms, we prepared PINK1 C-terminus (both HA- and c-Myc-tagged) constructs.

The data presented here regard the wild-type PINK1 protein and three mutants, two missense (G309D and A168P) and one nonsense (W437X) mutations. To exclude the possibility of nonsense-mediated transcript decay relative to the nonsense mutation, we confirmed the stability of the mutant transcript by semi-quantitative RT–PCR analysis on cells from heterozygous and homozygous carriers (data not shown).

Dual staining of transfected HeLa cells for wild-type PINK1 and for an abundant well-known mitochondrial protein, AFG3L2 (25), demonstrated the mitochondrial localization of PINK1 (Fig. 3A). The merged image for PINK1 (green) and AFG3L2 (red) revealed co-localization within mitochondria (overlap coefficient: $R_{over} = 0.675$). No signal was seen in mock-transfected HeLa cells (data not shown).

To exclude PINK1 localization in other organelles, we stained HeLa cells with anti-calnexin, an endoplasmic reticulum marker (Fig. 3B), and anti-LAMP1, a lysosomal marker (Fig. 3C). As shown, PINK1 does not co-localize with endoplasmic reticulum or lysosomal markers ($R_{over} = 0.321$ and 0.017, respectively). Similar results were obtained for $PINK1^{G309D}$, $PINK1^{A168P}$ and $PINK1^{W437X}$ mutants, suggesting that missense mutations in PINK1 protein, or loss of the C-terminus portion, do not alter its subcellular localization.

To confirm the effectiveness of the obtained R_{over}, we co-localized the two mitochondrial proteins AFG3L2 and TOM20 (a protein of the outer membrane). The R_{over} was 0.791 for the mitochondrial co-localization (Fig. 3D,

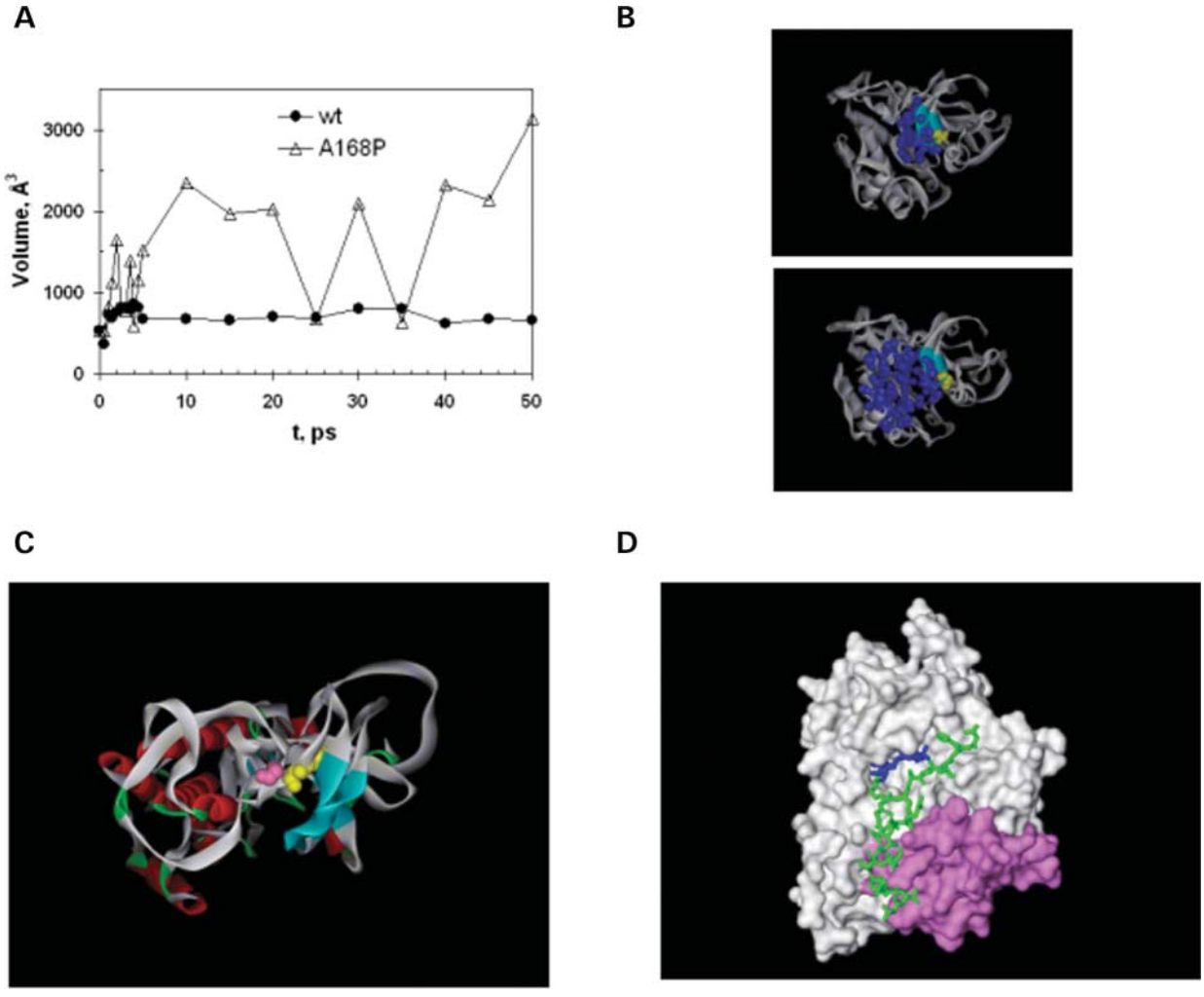

Figure 2. Protein modeling. (**A**) Volume of the protein cavity in the nucleotide phosphate-binding region as a function of simulation time. (**B**) Protein cavity in the nucleotide phosphate-binding region of the wild-type and the A168P mutant (left and right panels, respectively) at simulation time of 50 ps. The protein atoms that delineate the walls of the cavity are represented as dark blue spheres. The protein structure is rendered as gray ribbons, except the nucleotide phosphate residues 162–170 which is highlighted in light blue. Residue 168 is represented as yellow spheres. (**C**) Proximity of the catalytic lysine 186 (yellow spheres) with residue 309 (purple spheres). The protein is rendered as ribbons colored according to the secondary content (α-helices, red; β-sheets, light blue; coils, white; turns, green). (**D**) Model of the complex between PINK1 and a 20 amino acids residue substrate. PINK1 is represented as surface (residues 151–436 in white and residues 437–501 in purple), the substrate as green sticks and ATP as blue sticks.

upper panel) and 0.492 for the ER co-localization (Fig. 3D, lower panel).

PINK1 proteins are present in the mitochondrial-enriched fraction of mammalian cells

The mitochondrial localization of PINK1 was also verified by subcellular fractionation and immunoblotting. HeLa cells were fractionated by differential centrifugation, and the total lysate, the mitochondrial-enriched fraction and the cytoplasmic fraction were analyzed.

As shown in Figure 4A, two forms of PINK1, differing by approximately 10 kDa, were detected in total HeLa extracts. When we examined the subcellular fractions, we found that both bands were enriched in the mitochondrial-enriched fraction, and a similar enrichment of AFG3L2 was observed (Fig. 4A, lane 2). Very likely, smaller bands represented the mature forms obtained by cleavage of the LP. Only a residual fraction of PINK1 proteins was detected at the cytoplasmic level (Fig. 4A, lane 3).

No differences in the mitochondrial enrichment of $PINK1^{G309D}$ and $PINK1^{A168P}$ mutants were observed when compared with the wild-type protein, confirming that the tested missense mutations do not affect subcellular localization.

We confirmed that these results were not cell-type-specific by performing the same experiments in COS-7 cells (data not shown). We also verified that they were not influenced by the HA-tag by performing experiments with c-Myc-tagged proteins (data not shown).

Immunogold electron microscopy was used to better localize PINK1 inside mitochondria. As shown in Figure 4B, wild-type PINK1 protein (upper panel) or $PINK1^{W437X}$ (lower panel) localized on the mitochondrial cristae. The same results were obtained using $PINK1^{A168P}$ and $PINK1^{G309D}$ (data not shown).

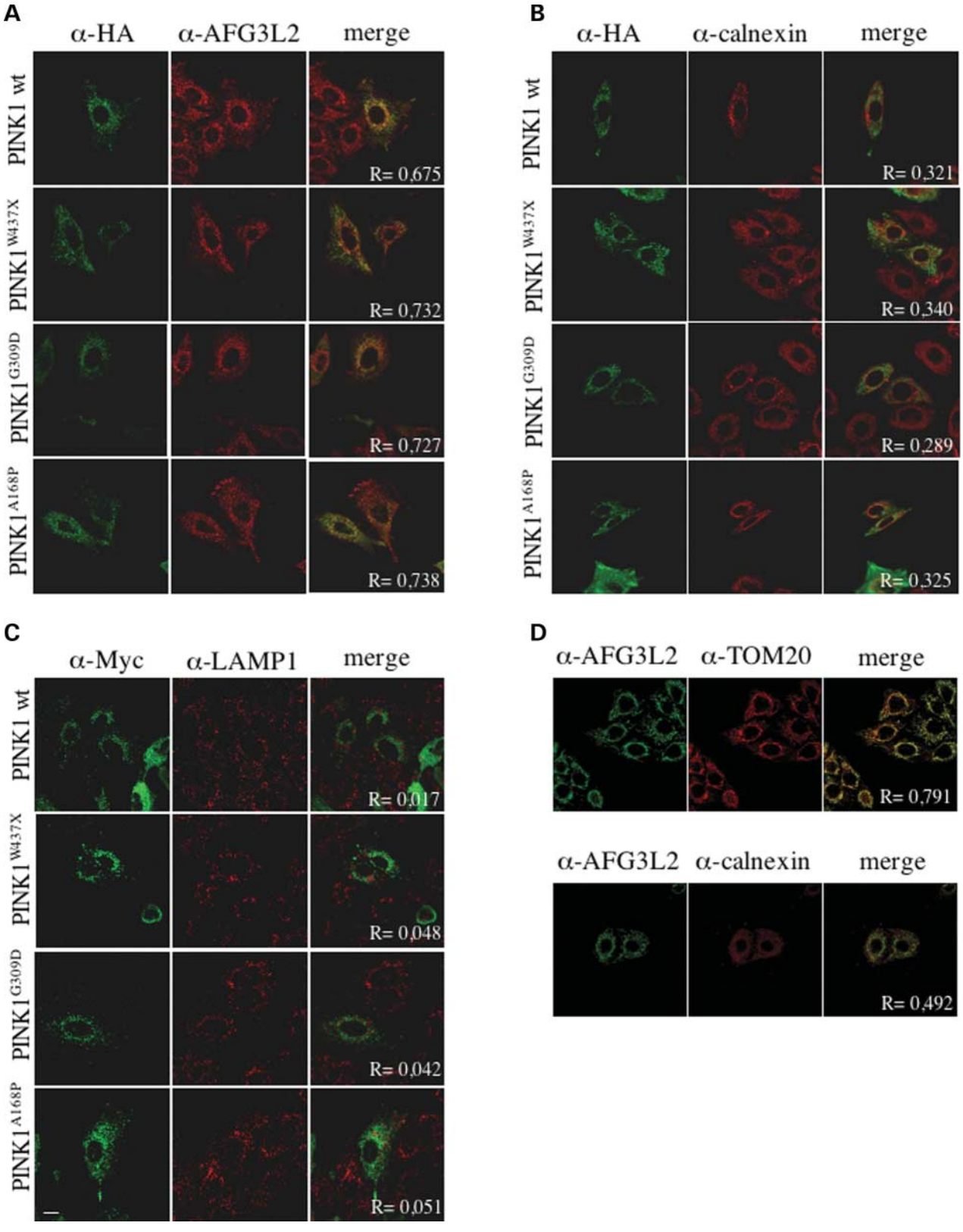

Figure 3. Mitochondrial localization of HA- or c-Myc-tagged PINK1 isoforms. (**A**) Confocal images of transfected HeLa cells representing PINK1-HA proteins (green) and AFG3L2 (red; mitochondria); merge pictures reveal co-localization. (**B**) PINK1-HA proteins are stained in green; endoplasmic reticulum (anti-calnexin antibodies) are visualized in red. (**C**) PINK1-Myc proteins (green); in red a marker for lysosomes (anti-Lamp1 antibodies). (**D**) Immunofluorescence of AFG3L2 positive cells (anti-TOM20, mitochondrial marker; anti-calnexin, endoplasmic reticulum marker). R represents the overlap coefficient. Scale bars: 10 μm.

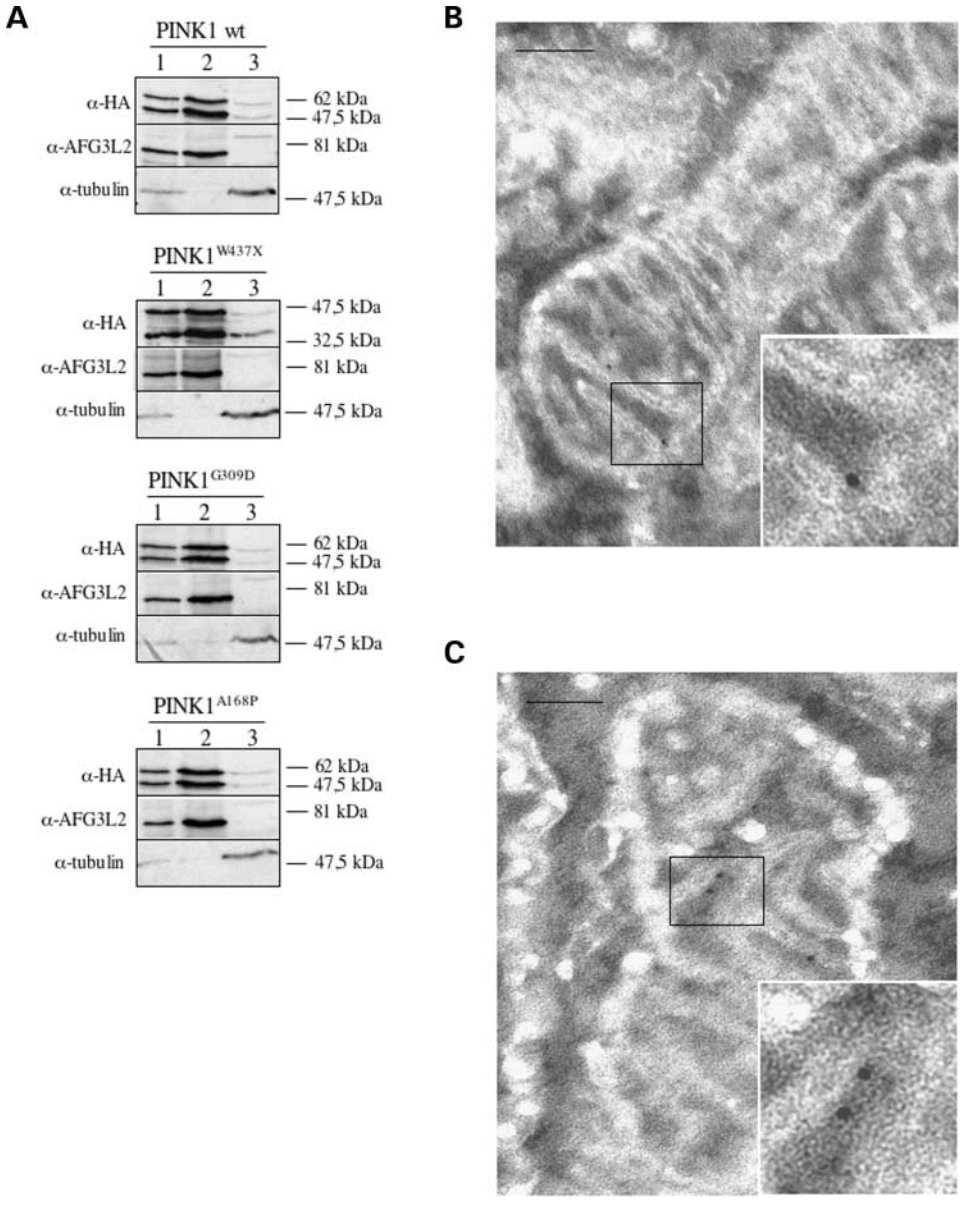

Figure 4. Subcellular localization and immunogold analysis of PINK1 proteins. (**A**) Western blot analysis of wild-type and mutant PINK1 proteins. 1, Total lysate; 2, mitochondrial-enriched fraction; 3, cytoplasmic fraction. AFG3L2 and α-tubulin were used as mitochondrial and cytoplasmic markers. (**B**) Immuno-electron microscopy of HeLa cells transfected with PINK1 proteins. HeLa cells were fixed and ultrathin sections were incubated with primary anti-HA antibody and secondary anti-IgG-coated gold particles. Upper panel: PINK1 wild-type; lower panel: PINK1^{W437X}. Scale bars: 200 nm.

PINK1 faces the mitochondrial intermembrane space

Immunoelectron microscopy suggested that PINK1 proteins are localized on mitochondrial cristae. To determine whether PINK1 is exposed to the intermembrane space or enclosed within the matrix, we combined digitonin extractions with protease digestions (Fig. 5). Digitonin disorganizes the outer membrane, making intermembrane space proteins accessible to cleavage by exogenously added proteases such as trypsin. As a control, protease sensitivity of the integral protein TIM23 of the inner mitochondrial membrane was assessed. Wild-type PINK1 (Fig. 5A) and PINK1^{W437X} (Fig. 5B) were also digested in the presence of digitonin, thereby indicating that PINK1, or at least its HA-tagged C-terminus, is possibly exposed to the intermembrane space. The α-subunit of F_1F_0 ATP synthase was not affected by trypsin in this condition.

Wild-type and mutant PINK1 are *in vitro* imported into mammalian mitochondria with the same efficiency

To confirm the mitochondrial internalization and cleavage of PINK1 preprotein to the shorter mature form, *in vitro*-translated PINK1 precursors were incubated in the presence of isolated human mitochondria. Import into mitochondria was assayed by two criteria: (i) cleavage of the signal sequence and (ii) sedimentation of the imported molecules

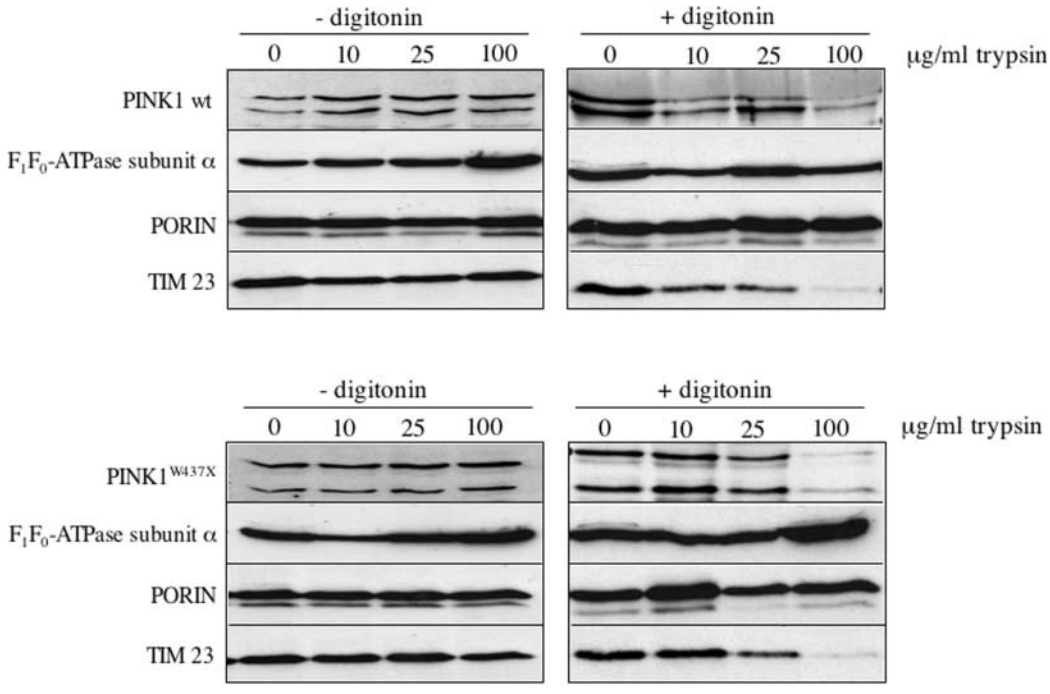

Figure 5. Protease protection assay. Accessibility to protease digestion as determined by treating mitochondria with digitonin and increasing concentrations of trypsin. After 30 min, the reaction was stopped by adding TCA, and the proteins were analyzed by SDS–PAGE and western blotting. Porin is an outer mitochondrial membrane. TIM23 localizes on the inner mitochondrial membrane and faces the intermembrane space. F_1F_0 ATPase is an inner membrane protein and faces the matrix.

with mitochondria by centrifugation. Wild-type and mutant PINK1 proteins were actively imported into mitochondria (Fig. 6) and the preproteins were processed to a mature form (m) of about 55 kDa (wild-type PINK1, PINK1^{G309D} and PINK1^{A168P}) and to a mature form of about 40 kDa for the PINK1^{W437X} truncating variant, consistent with the sizes observed on immunoblots. Import and maturation were efficient for both wild-type and mutant proteins. Proteinase K treatment of mitochondria incubated with PINK1 proteins demonstrated that both the preprotein and the mature forms were present inside the mitochondria and that only a small amount of the preprotein was digested by protease treatment.

The requirement of an inner membrane potential for protein internalization was evaluated by using the respiratory chain uncoupler valinomycin. PINK1 protein import was abolished in mitochondria exposed to valinomycin, as demonstrated by the lack of the corresponding mature forms.

The ambiguity of the localization of the cleavage site by prediction analysis—two possible sites were identified at position 35 (MitoProt) and at position 77 (TargetP)—was substantially solved: the longer 8.5 kDa LP released by cleavage at position 77 is consistent with our experimental data.

Solubility of PINK1 proteins

PINK1 protein features an elevated isoelectric point (9.46) and a high mean value of hydrophobicity [−0.018; GRAVY (26)]. In addition, the presence of a transmembrane domain at positions 101–107 (DAS-Transmembrane Prediction Server) classifies PINK1 as an integral membrane protein. Integral membrane proteins exhibit different solubility when compared with soluble proteins. To characterize the solubility properties of wild-type and mutant PINK1 proteins, HeLa cells were transiently transfected with pcDNA3.1 constructs expressing the wild-type protein and three mutants (PINK1^{W437X}, PINK1^{G309D} and PINK1^{A168P}, Fig. 7).

Twenty-four hours after transfection, cells were harvested and proteins were differentially extracted as described in Materials and Methods, using non-ionic (Triton X-100, Fig. 7A), zwitterionic (CHAPS, Fig. 7B), surfactant-like (digitonin, Fig. 7C) and anionic (Sarkosyl, Fig. 7D) detergents.

Wild-type and mutant variants of PINK1 were present in the detergent-insoluble fractions obtained after treatment with Triton, CHAPS and digitonin. However, after Sarkosyl treatment, PINK1 proteins were recovered in the soluble fractions. In 0.1% Sarkosyl, the AFG3L2 protein was present in the soluble fraction, but PINK1 was completely solubilized only at 0.5%. However, by closer observation, small amount of PINK1 corresponding mainly to the precursor form was solubilized in 0.1% Sarkosyl, whereas the mature form appeared to be more tightly interact with membranes. Wild-type and mutant proteins exhibited the same solubility, suggesting that PINK1 is naturally prone to adopting detergent-insoluble conformations or to aggregate in partially insoluble structures.

The N-terminal part of PINK1 is sufficient for its mitochondrial localization

To confirm that the N-terminal portion of PINK1 is responsible for its mitochondrial localization, two chimeric proteins

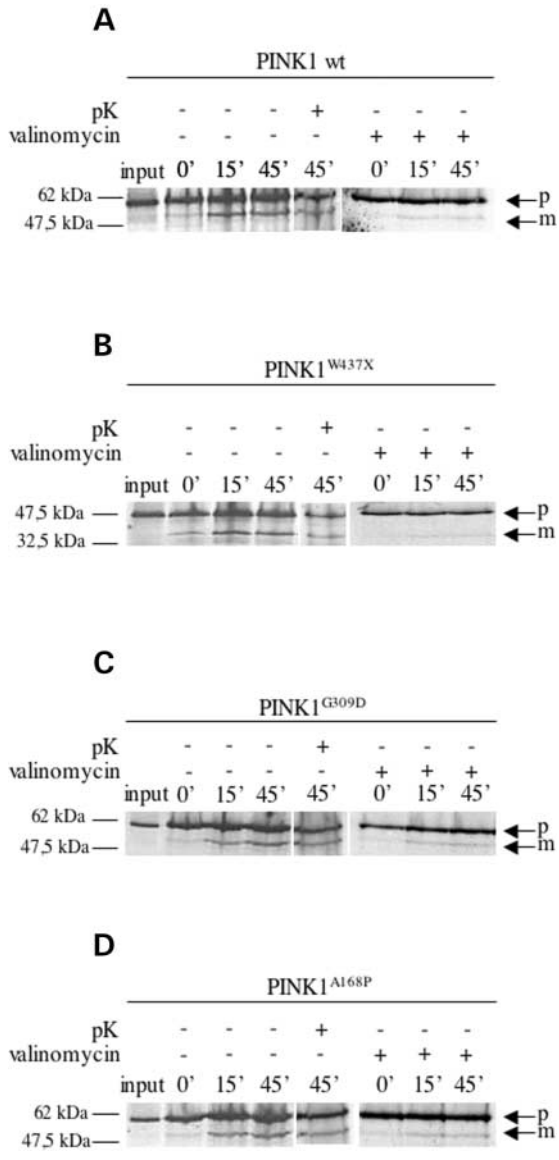

Figure 6. *In vitro* mitochondrial import of wild-type and mutant PINK1 proteins (p, precursor; m, mature). (**A**) wild-type PINK1; (**B**) PINK1^{W437X}; (**C**) PINK1^{G309D}; (**D**) PINK1^{A168P}. The mitochondrial potential $\Delta\Psi$ was dissipated using valinomycin.

(LP-ECFP and LP-TM-ECFP) were constructed, in which the presequence of the human PINK1 precursor (LP, for leader peptide; and LP-TM, for leader peptide and transmembrane domain) were fused to a fluorescent protein (Fig. 8A).

In cells expressing ECFP, fluorescence was distributed throughout the cell including the nucleus (data not shown). In contrast, in cells expressing LP-ECFP or LP-TM-ECFP, strong particulated fluorescence characteristic of mitochondria were observed (Fig. 8B). LP-ECFP and LP-TM-ECFP were visualized for ECFP and for the endogenous TOM20 using immunocytochemical analysis. The pattern of LP-ECFP and LP-TM-ECFP coincided with that of the TOM20 stain ($R_{over} = 0.821$ and 0.794, respectively). This result demonstrates that the N-terminus of PINK1 protein is sufficient for its mitochondrial localization.

The intracellular localization of LP-TM-ECFP protein and its processing were also analyzed by cell fractionation (Fig. 8C). In cells expressing ECFP, a larger portion of ECFP protein was recovered in the cytoplasmic fraction (data not shown). When LP-TM-ECFP was expressed, the processed mature LP-TM-ECFP was detected mainly in the mitochondrial-enriched fraction (lane 2), where it represented approximately 30% of the precursor, and was not present in the cytoplasmic fraction (lane 3).

The insolubility properties of PINK1 protein were not retained in the chimeric construct and, as shown in Figure 8D, LP-TM-ECFP was soluble at low concentration of Triton X-100.

PINK1^{W437X} autophosphorylates more efficiently than wild-type and missense mutants

Protein domain prediction analysis of PINK1 protein identified a conserved serine–threonine kinase domain, which spans from amino acid 156 to amino acid 509. The kinase domain of PINK1 is able to autophosphorylate, as reported previously (8). To assess the kinase activity of wild-type and PARK6 mutants, we obtained GST-PINK1 fusion proteins. The chimeric proteins lacked the 112 amino acid fragment at the N-terminus were responsible for PINK1 aggregation in bacteria (8); this region comprises the mitochondrial LP (amino acids 1–77) and the putative transmembrane domain (amino acids 101–107). PINK1 proteins were purified on a glutathione-Sepharose column, and assayed by SDS–PAGE and Coomassie staining as a single 77 kDa polypeptide for wild-type and missense mutants, and a single 61 kDa polypeptide for PINK1^{W437X} mutant, consistent with predicted molecular masses of fusion proteins (Fig. 9B).

The same stoichiometric amount of PINK1 proteins was incubated in kinase buffer in the presence of [γ-^{32}P]ATP. As shown in Figure 9, GST-fused PINK1 proteins were able to autophosphorylate *in vitro*. However, GST-PINK1^{W437X} (lane 2) autophosphorylated more efficiently than the wild-type (lane 1) and the missense mutants (PINK1^{G309D}, lane 3 and PINK1^{A168P}, lane 4). The autophosphorylation of wild-type PINK1, PINK1^{A168P} and PINK1^{G309D} showed the same efficiency, suggesting that missense mutations do not impair this ability.

When PINK1 wild-type and PINK1^{W437X} proteins were incubated together (lane 1 and 2), in the presence of [γ-^{32}P]ATP, the intensity of the bands corresponding to proteins were more intense, probably due to the increased protein concentration.

Furthermore, we tested PINK1 kinase activity on a general substrate protein by incubating GST-fusion proteins in the presence of α-casein. As shown in Figure 10, wild-type PINK1 (lane 1), PINK1^{W437X} (lane 2), PINK1^{G309D} (lane 3) and PINK1^{A168P} (lane 4) mutants exhibited the same efficiency in phosphorylating α-casein.

The C-terminal peptide of PINK1 down-regulates autophosphorylation

Considering the higher autophosphorylation activity of GST-PINK1^{W437X} when compared with wild-type and mutant

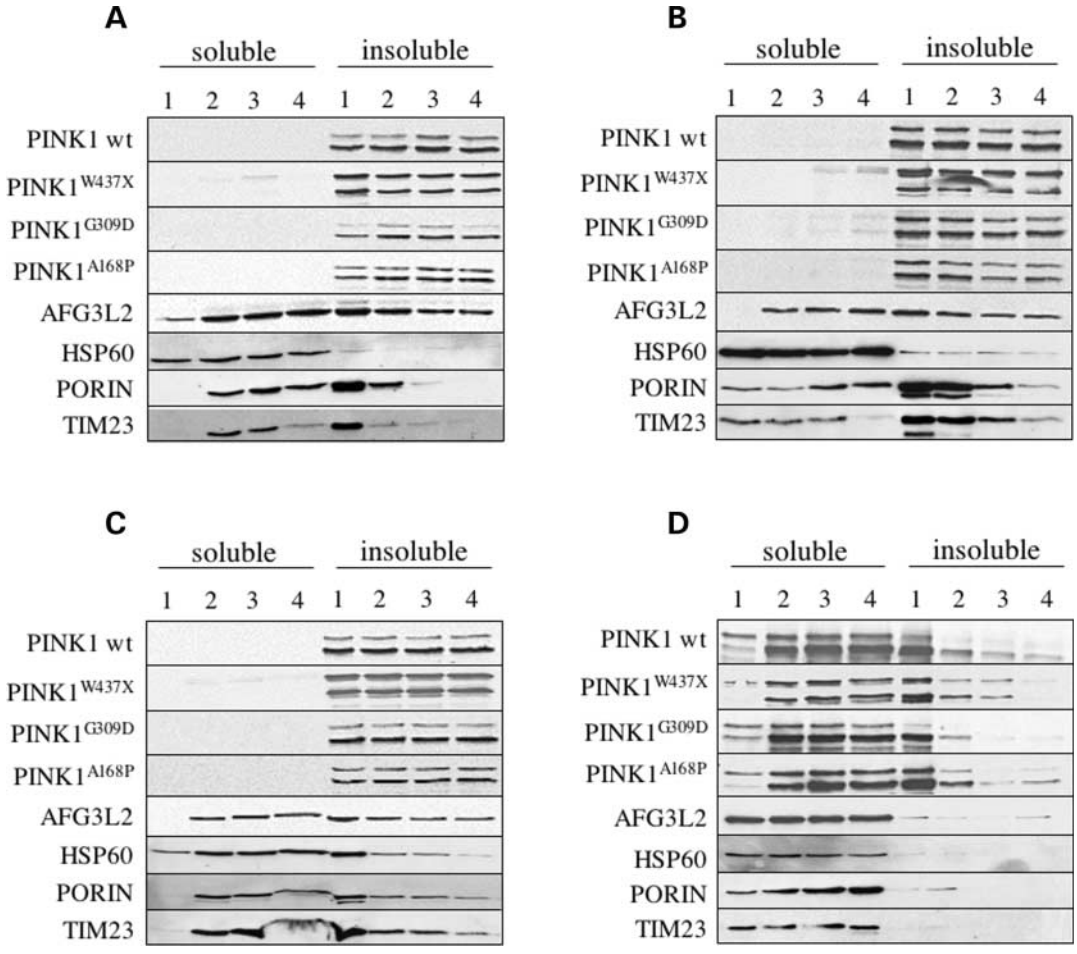

Figure 7. PINK1 detergent solubility. Mitochondria from transfected HeLa cells were treated with 0.1% (lane 1), 0.5% (lane 2), 2% (lane 3), 5% (lane 4) of Triton X-100 (non-ionic, **A**), CHAPS (zwitterionic, **B**), digitonin (surfactant-like, **C**) and Sarkosyl (anionic, **D**). After centrifugation, the supernatant was the detergent-soluble fraction and the pellet was the detergent-insoluble fraction. AFG3L2, HSP60, porin and TIM23 were used to follow protein solubilization.

proteins (Fig. 9), we hypothesized that the C-terminus peptide of the protein might negatively regulate its enzymatic activity. To test this hypothesis, we isolated the kinase domain of PINK1 (amino acids 112–496) and obtained GST-fusion proteins (GST-PINK1-*KD*, kinase domain only). Recombinant proteins were purified and assayed by SDS–PAGE and Coomassie staining as a 67 kDa polypeptide for wild-type and missense mutants (Fig. 11B). Same stoichiometric amounts of wild-type and PARK6 mutant proteins were independently incubated in the presence of labeled ATP.

As shown in Figure 11, the GST-PINK1-*KD*, which expresses wild-type PINK1 kinase domain (lane 2), autophosphorylated more efficiently than the full-length protein (GST-PINK1, lane 1), suggesting that the peptide from 496 to 581 has a negative regulatory role. Also, the GST-PINK1-KD^{G309D} (lane 5) and the GST-PINK1-KD^{A168P} (lane 7) showed an increased autophosphorylation rate when compared with the corresponding full-length (lanes 4 and 6, respectively). However, we observed a reduction of autophosphorylation by comparing the activity of mutant proteins to the wild-type (lanes 3, 5 and 7 against lane 2). In particular, the G309D mutation affects the autophosphorylation activity more than A168P and W437X mutations.

Kinase activity toward a heterologous substrate was tested in the presence of α-casein and the results are shown in Figure 12. Mutant and wild-type proteins, with or without the C-terminal peptide, phosphorylated α-casein with comparable efficiency. No differences were seen between wild-type (lane 2) and mutant proteins (PINK1-KD^{W437X}, lane 3; PINK1-KD^{G309D}, lane 5; PINK1-KD^{A168P}, lane 7), also in the presence of different efficiency of autophosphorylation. Possibly, in the presence of the still unknown natural substrates, PINK1 mutants exhibit abnormal kinase activity.

DISCUSSION

Mitochondrial dysfunction has been linked to several neurodegenerative conditions in the last decades. Besides mitochondrial diseases originating from mutations of the organellar genome, numerous nuclear-encoded genes have recently been associated to hereditary spastic paraplegia (27),

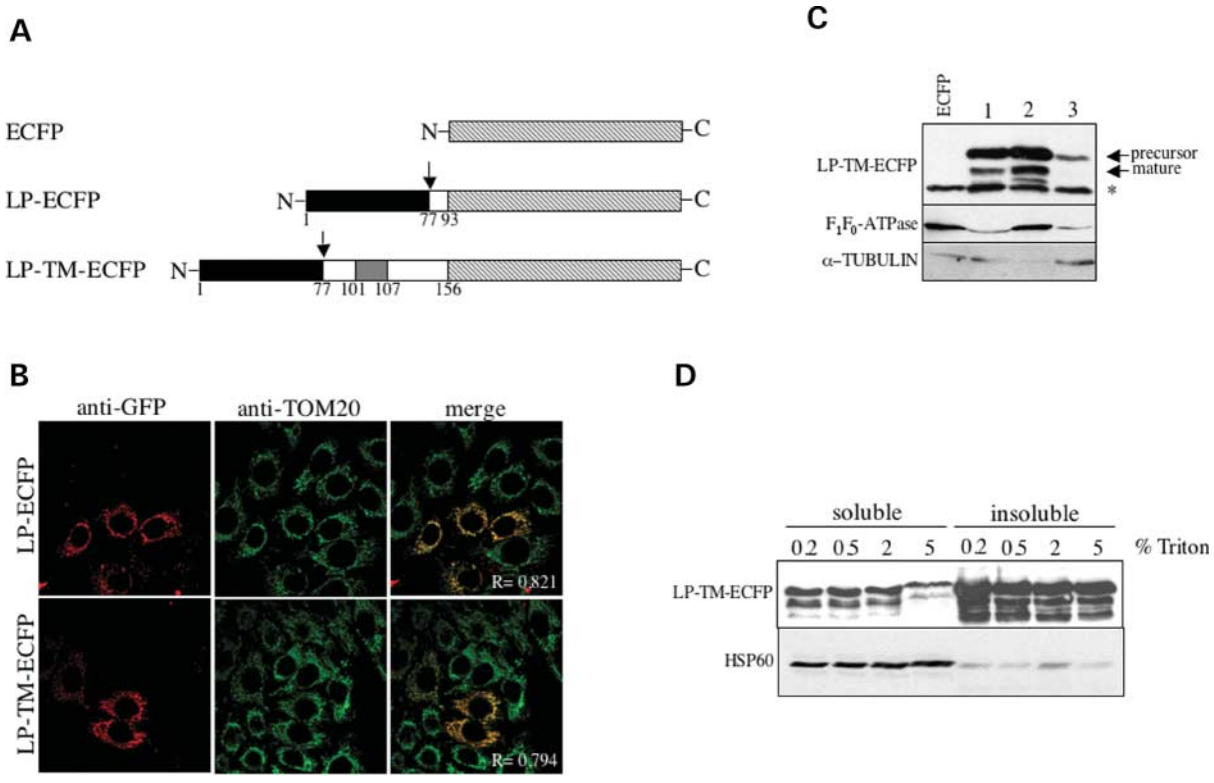

Figure 8. ECFP was specifically targeted to the mitochondria by fusing PINK1 N-terminal domains. (**A**) Schematic representation of chimeric proteins resulting from the fusion of the first 93 (including the LP) or 153 amino acids (LP plus transmembrane domain, LP-TM) of PINK1 protein in frame with the ECFP. Black box, the LP; gray box, the TM domain; the dashed boxes show the ECFP. (**B**) Confocal analysis of LP-ECFP- and LP-TM-ECFP-transfected HeLa cells; in red, anti-GFP antibody recognizing ECFP fusion proteins; in green, anti-TOM antibody (mitochondrial marker). (**C**) Subcellular fractionation of HeLa cells transfected with LP-TM-ECFP. 1, Total lysate; 2, mitochondrial-enriched fraction; 3, cytoplasmic fraction. F_1F_0-ATPase of complex V and α-tubulin was used as mitochondrial and cytoplasmic markers; *ECFP is due to the presence of the ECFP start codon, which remains downstream the LP-TM sequence. (**D**) LP-TM-ECFP solubility. Mitochondria from transfected HeLa cells were treated with increasing concentration of Triton X-100. After centrifugation, the supernatant was the detergent-soluble fraction and the pellet was the detergent-insoluble fraction. HSP60 was used to follow protein solubilization.

Friedreich ataxia, Leigh syndrome, Wilson disease, amyotrophic lateral sclerosis (28), Mohr-Tranebjaerg syndrome (29), Alzheimer disease and Huntington disease (30).

Among the known genes responsible for familial and sporadic forms of parkinsonism, PARK6-associated PINK1 is the only gene product directly targeted to the mitochondria. The original evidence showing a mitochondrial localization of PINK1 has been obtained with an amino-terminus-tagged protein that partially masks the mitochondrial LP, possibly altering the natural targeting of the protein. A recent paper confirmed the mitochondrial processing and localization of PINK1, but showed a possible cytoplasmic localization of the processed PINK1 protein in COS-7 cells by both immunofluorescence and subcellular fractionation (31). Here, we present data demonstrating and confirming the mitochondrial tropism of wild-type and different PARK6 mutant forms of PINK1.

Immunofluorescence analysis of the carboxy-tagged PINK1, mitochondrial protein fractionation, electron microscopy and *in vitro* import experiments clearly demonstrated that PINK1 is a nuclear-encoded mitochondrial protein. During the mitochondrial import of *in vitro*-labeled PINK1, the LP cleavage in position 77 is preferred to the predicted one at position 35 and gives reason for the appearance of two forms of PINK1, the preprotein and the mature one, differing by approximately 10 kDa. This is in line with results by Beilina *et al*. (31), who also observed a processed protein about 10 kDa smaller, for both wild-type and two missense mutant proteins.

PINK1 preproteins are quite represented within the mitochondria, suggesting that the LP has not yet been cleaved from the translocase of outer/inner membrane complex, as it seems the case of a relevant portion of mitochondrial proteins (32). In particular, the protease protection assay unequivocally demonstrated that both the preprotein and the mature form of PINK1 expose the C-terminus to the intermembrane space. All tested proteins, including the wild-type, the truncating W437X and the missense G309D and A168P polypeptides behave similarly, therefore indicating that PINK1 mutants are efficiently imported into mitochondria, where they exert their bona fide pathogenic role.

To demonstrate unequivocally that the N-terminus of PINK1 is sufficient for its mitochondrial targeting, we constructed chimeric ECFP proteins with the N-terminal part of PINK1 and analyzed their mitochondrial localization, processing and biochemical features by a combination of fluorescence microscopy, cell fractionation, immunoblot

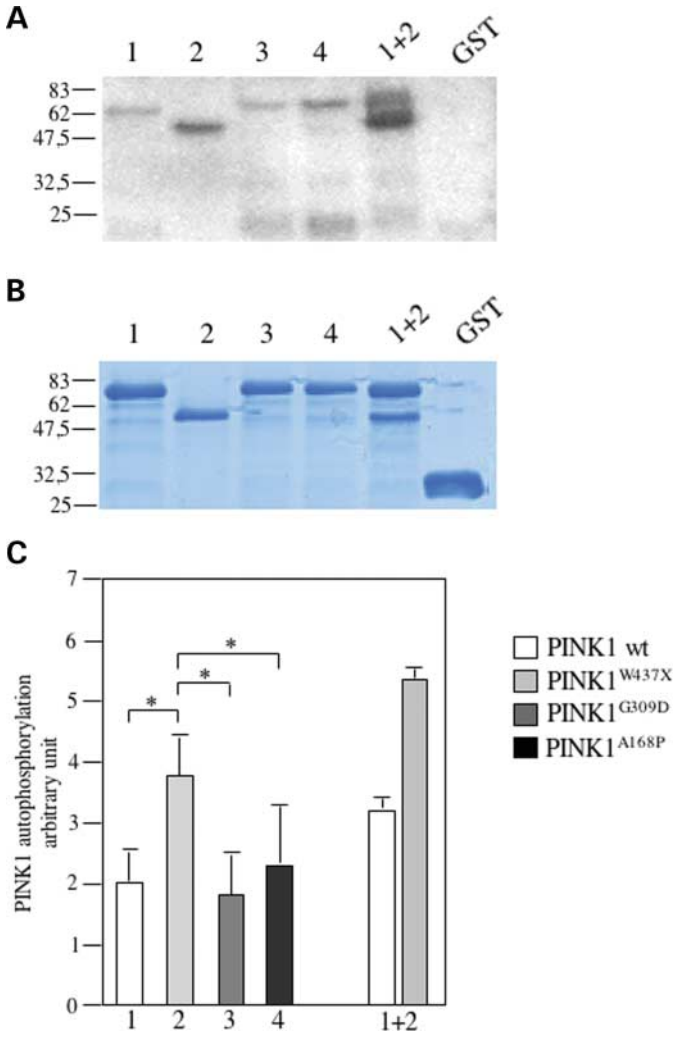

Figure 9. Autophosphorylation of full-length PINK1 proteins. GST-fused PINK1 proteins were incubated with [γ-^{32}P]ATP. (**A**) Autoradiography of GST-PINK1 proteins: 1, GST-PINK1 wild-type; 2, GST-PINK1^{W437X}; 3, GST-PINK1^{G309D}; 4, GST-PINK1^{A168P}; GST, control GST protein from induced empty vector; (**B**) Coomassie staining; (**C**) normalized autophosphorylation levels. Error bars, S.E. of three independent experiments. $^{*}P < 0.05$.

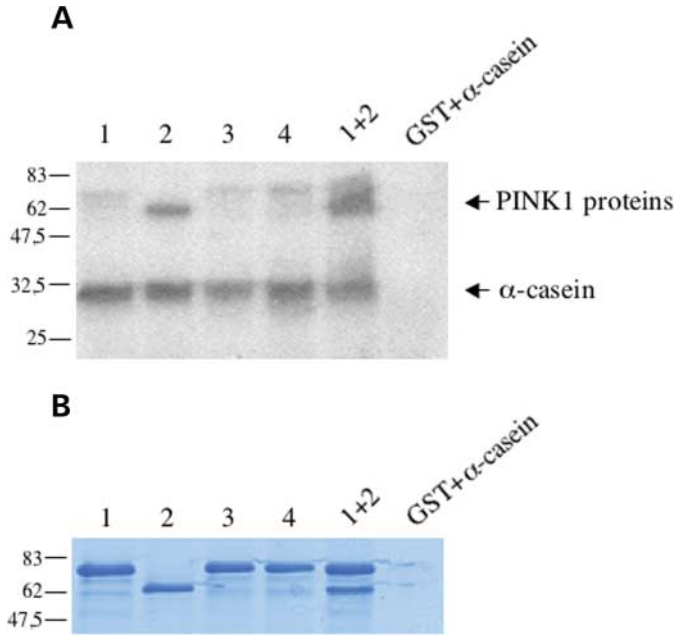

Figure 10. α-Casein phosphorylation by full-length PINK1 isoforms. GST-fused PINK1 proteins were incubated with [γ-^{32}P]ATP in the presence of α-casein. (**A**) Autoradiography of α-casein and GST-PINK1 proteins: 1, GST-PINK1 wild-type; 2, GST-PINK1^{W437X}; 3, GST-PINK1^{G309D}; 4, GST-PINK1^{A168P}; (**B**) Coomassie staining.

analysis and detergent solubility. We showed that small amino-terminal portions of PINK1 were sufficient to correctly target chimeric proteins to the mitochondria. In addition, one of these fusion proteins, LP-TM-ECFP, accumulated in the mitochondrial-enriched fraction and was processed into a mature form.

The presence of a predicted trans-membrane domain, together with cell fractination experiments, may suggest that PINK1 is an integral mitochondrial protein. Mitochondrial membranes host core processes of the organelle and harbor hundreds of proteins displaying a large range of isoelectric points (i.e. as acidic as 4.5 to basic 11; PINK1 i.p. is 9.4). We could solubilize PINK1 protein only by using anionic detergents, whereas different kinds of detergents failed to bring PINK1 in the soluble fraction. These detergents, including non-ionic, zwitterionic and surfactant-like detergents, have proved effective in solubilizing model integral proteins, in particular, the chimeric protein LP-TM-ECFP. This data suggest that the kinase domain of PINK1 is highly hydrophobic and tightly associated to the mitochondrial membranes and that it is the major cause of PINK1 insolubility. This observation applies to both wild-type and PARK6 mutants. The insolubility of PINK1 could also be explained by local differential lipid composition. A characteristic feature of the plasma membrane is the presence of lipid rafts, which represent sort of delimitated chambers, where several subcellular activities take place; in fact, lipid raft proteins show detergent insolubility. Recently, it has been proposed that lipid microdomains exist also in mitochondria, where the GD3 molecule create a close chamber, a specialized portion of mitochondrial membranes contributing to the instruction of the apoptotic execution cascade (33).

Sequence homology, MD and structural fitting simulations recognize PINK1 as a serine–threonine kinase. Most frequently, the occurrence of (auto)phosphorylation of the activation loop of the kinase domain unmasks the catalytic site that starts transferring the phosphate moiety to the substrate.

Contrary to the generally expected loss-of-function effect for a recessive variant, our data demonstrate that the truncating W437X mutant autophosphorylates more efficiently than the other full-length isoforms, including wild-type and the two missense mutants.

We therefore postulated a possible role of PINK1 C-terminal portion in the regulation of the autophosphorylation process. We tested an additional series of constructs expressing wild-type and the two missense mutants removed of the C-terminal regulatory sequence responsible, in most cases, of the specific recognition of the substrate (34) and demonstrated that wild-type PINK1 autophosphorylation is more efficient than mutant isoforms activity, confirming the

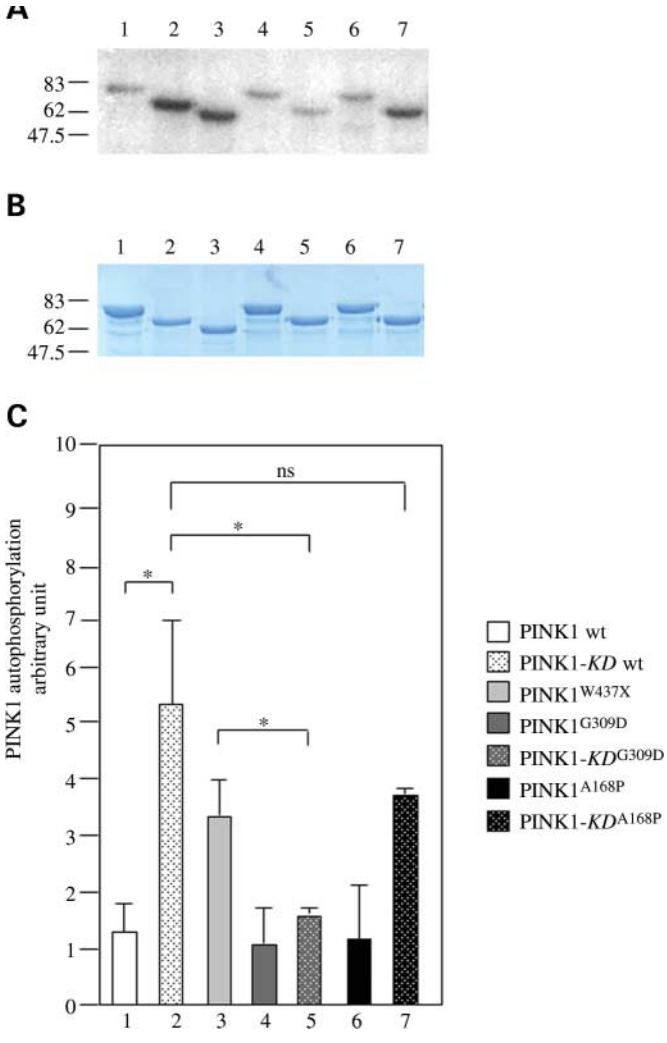

Figure 11. PINK1 C-terminal peptide regulates autophosphorylation. (**A**) Autoradiography of GST-PINK1 proteins: 1, GST-PINK1 wild-type; 2, GST-PINK1-*KD*; 3, GST-PINK1^{W437X}; 4, GST-PINK1^{G309D}; 5, GST-PINK1-*KD*^{G309D}; 6, GST-PINK1^{A168P}; 7, GST-PINK1-*KD*^{A168P}; (**B**) Coomassie staining; (**C**) normalized autophosphorylation scores. KD, kinase domain only. Error bars, S.E. of three independent experiments. $^{*}P > 0.05$.

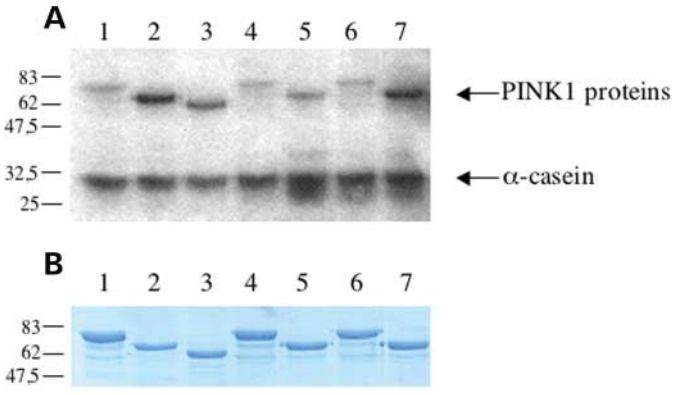

Figure 12. PINK1 kinase domain is sufficient to phosphorylate α-casein. (**A**) Autoradiography of α-casein in the presence of: 1, GST-PINK1 wild-type; 2, GST-PINK1-*KD*; 3, GST-PINK1^{W437X}; 4, GST-PINK1^{G309D}; 5, GST-PINK1-*KD*^{G309D}; 6, GST-PINK1^{A168P}; 7, GST-PINK1-*KD*^{A168P}; (**B**) Coomassie staining.

findings of Beilina *et al*. (31). If we assume autophosphorylation efficiency as an index of kinase activity, mutant isoforms should display minor or absent kinasing activity, which fits with the expected loss-of-function model typical of recessive diseases.

Nevertheless, the *in vitro* kinase activity of all constructs directed toward an external general substrate such as α-casein is very similar. However, this quite basic test just describes the kinase potential of the tested protein, whereas a specific comparison of PINK1 kinase activity between wild-type and mutant proteins should be carried out in the presence of the still unknown natural PINK1-specific substrate. It can be hypothesized that, similar to DJ-1, PINK1 acts as a stress-induced protein which can exert its kinase activity only when the regulatory effect of the C-terminus on protein autophosphorylation is removed under specific cellular conditions, still unknown at present.

Numerous mitochondrial proteins involved in the main mitochondrial activities, namely steroidogenesis, fatty acid metabolism and oxidative phosphorylation, are phosphoproteins (35). Although our knowledge on protein kinases directed to the mitochondria through a canonical LP is poor and incomplete, several kinases translocate to the mitochondrion from other subcellular compartments under challenging environmental conditions or following signaling cascade inputs. In fact, protein kinase A targeted to mitochondria localizes to the matrix and inner membrane where it exerts a positive regulation of complex I activity (36). Differently, protein kinase Cδ translocation to mitochondria is proapoptotic by devastating the mitochondrial membrane potential and promoting cytochrome C release (37).

At present, we reckon that PINK1 function can be linked to PARK6 pathogenesis by two main hypotheses involving energy deficit and/or apoptotic cascade. Several respiratory complex subunits need phosphorylation to ensure correct assembly and activity of complexes and PINK1 may directly or indirectly provide for a portion of these post-translational modifications. Decreased or null activity of mutant PINK1 would negatively affect ATP synthesis and the whole cellular energetic capacity. Possible outcomes of this impairment in dopaminergic neurons include unbalance of ion gradient homeostasis regulated by the Na–K pump, which utilizes a large fraction of the available ATP and is massively expressed in this cells, thus compelling neurons to degeneration (38). An additional energy-consuming system is represented by the proton pump located on synaptic vesicles. Upon decreased activity of proton pump function, dopamine diffuses into the cytoplasm where, beside its direct inhibition of respiratory complex I, it greatly contributes to enhancing the overall oxidative stress potential, even by means of its metabolite DOPAC (39).

In contrast, by failing to phosphorylate physiologic substrates, mutant PINK1 isoforms may trigger the signaling cascade leading to the opening of the permeability transition pore, hence commencing the mitochondrial way to apoptosis by both caspase-dependent and -independent mechanisms (40). Although more functional information are needed to

properly trace the series of molecular events stemming from PINK1 mutant dysfunction and leading to substantia nigra neuron degeneration, the primary role of mitochondria is getting on focus.

MATERIALS AND METHODS

Cell cultures

HeLa and COS-7 cells were cultured in Dulbecco's modified Eagle's medium (DMEM; Invitrogen, Carlsbad, CA), supplemented with 2 mM L-glutamine, 200 U/ml penicillin, 200 μg/ml streptomycin, 1 mM sodium pyruvate and 10% heat-inactivated FBS at 37°C in 95% humidifier air and 5% CO_2.

PINK1 expression constructs

pcDNA3.1-PINK1-HA/Myc. The whole PINK1 open reading frame omitting the stop codon was amplified from the human cDNA by using primers 5′-cccaagcttaccatggcggtgc gacag-3′ (sense; *Hin*dIII tail) and 5′-ggaattccagggctgccctc catga-3′ (antisense; *Eco*RI tail) and cloned into the *Hin*dIII and *Eco*RI sites of pcDNA3.1(+) (Invitrogen).

To introduce the HA or the c-Myc tags into the C-terminus of Pink1, the pcDNA3.1-PINK1 plasmid was digested with *Eco*RI and *Xho*I and the HA or c-Myc oligonucleotides were cloned to obtain the pcDNA3.1-PINK1-HA and the pcDNA3.1-PINK1-Myc plasmids. Oligonucleotides were 5′- and 3′-modified for the cloning strategy and the stop codons were inserted into the sequences.

The sequences of the HA primers were: 5′-aattctacccatac gatgttccagattacgcttgac-3′ (sense) and 5′-tcgagtcaagcctaatctg gaacatcgtatgggtag-3′ (antisense); the sequences of the c-Myc primers were: 5′-aattcgagcaaaagctgatttctgaggaggatctgtgac-3′ (sense) and 5′-tcgagtcacagatcctcctcagaaatcagcttttgctcg-3′ (antisense).

pcDNA3.1-PINK1^{W437X}-HA/Myc. To introduce the stop mutation at position 437, we amplified a truncated fragment of pcDNA3.1-PINK1 using oligonucleotides 5′-cccaagcttac catggcggtgcgacag-3′ (sense; *Hin*dIII tail) and 5′-ggaattcggcat cagccttgctgtagtc-3′ (antisense; *Eco*RI tail). The HA- and c-Myc tags were inserted using the strategy described above.

pcDNA3.1-PINK1^{G309D}-HA/Myc. The glycine residue at position 309 of Pink1 was changed to an aspartic acid residue using the QuickChange site-directed mutagenesis kit (Stratagene, La Jolla, CA) according to the manufacturer's protocol. The plasmid pcDNA3.1-PINK1 was used as template and the method required two oligonucleotides; 5′-accctgaaggcctggaccatggccggacgct-3′ (sense) and 5′-agcg tccggccatggtccaggccttcagggt-3′ (antisense).

pcDNA3.1-PINK1^{A168P}-HA/Myc. The alanine residue at position 168 of PINK1 was mutated to a proline residue as described above using oligonucleotides 5′-cattggtaagggctg cagtcctgctgtgtatgaagccaccatg-3′ (sense) and 5′-catggtggcttca tacacagcaggactgcagcccttaccaatg-3′ (antisense).

pcDNA3.1-LP-ECFP and pcDNA3.1-LP-TM-ECFP. The cDNA sequences corresponding to the LP (amino acids 1–93) and the leader plus the putative transmembrane domain of PINK1 (LP-TM, amino acids 1–156) were amplified, *Hin*dIII and *Bam*HI digested and cloned in frame with the N-terminus of ECFP (pECFP-N1 vector, Stratagene). The primers were as follows: 5′-cccaagcttaccatggcggtgcgacag-3′ (sense; *Hin*dIII tail); for the LP only: 5′-gcggatccgcgcagccc caggcccgcac-3′ (antisense; *Bam*HI tail); for the LP-TM: 5′-gcggatcctcctccagccgaaagcc-3′ (antisense; *Bam*HI tail). The resulting vectors (pECFP-N1-LP and pECFP-N1-LP-TM) were digested with *Hin*dIII and *Not*I, to excise the PINK1 N-terminal sequences and the ECFP, and cloned into pcDNA3.1(+) (Invitrogen) (pcDNA3.1-LP-ECFP and pcDNA3.1-LP-TM-ECFP).

GST-fused proteins. cDNA fragments covering the 112–581 amino acid residues were amplified from plasmids pcDNA3.1-PINK1, pcDNA3.1-PINK1^{G309D} and pcDNA3.1-PINK1^{A168P} using oligonucleotides 5′-cgggatccgaggaaaaa caggcggag-3′ (sense; *Bam*HI tail) and 5′-ggaattctcacagggct gccctccatga-3′ (antisense; *Eco*RI tail) and cloned into the *Bam*HI–*Eco*RI sites of the pGEX4T1 vector (Amersham Biosciences AB Pharmacia Biotech), in frame with the GST protein. The 112–496 amino acid residues for PINK1-*KD*, PINK1-*KD*^{G309D} and PINK1-*KD*^{A168P}, covering the kinase domain (*KD*) of PINK1 proteins, were amplified using the sense oligonucleotide described above and the antisense oligonucleotide, *Eco*RI tail, 5′-ggaattct-cacttgctggcctctcgctg-3′. Fragments were cloned into the *Bam*HI–*Eco*RI sites of the pGEX4T1 vector.

To generate the GST-fused protein PINK1^{W437X}, the 112–437 amino acid residues were amplified from pcDNA3.1-PINK1 vector with the sense oligonucleotide described earlier and the antisense, *Eco*RI tail oligonucleotide 5′-ggaattcggcatcagccttgctgtagtc-3′, and the fragment was cloned in pGEX4T1 vector.

The *Escherichia coli* strain XL-10 Gold was transformed with plasmids. After 3 h of induction with 0.1 mM isopropyl thiogalactopyranoside (Sigma), the GST-PINK1 fusion proteins were purified with glutathione-Sepharose 4B (Amersham Biosciences AB Biosciences AB, Uppsala, Sweden) according to the manufacturer's instructions. Protein preparations were analyzed by Coomassie staining of SDS–PAGE, under standard conditions.

Isolation of mitochondria

Mitochondria were isolated by differential centrifugation of HeLa and COS-7 cell homogenates (41). In brief, cells were washed in PBS, resuspended in an appropriate isotonic buffer (0.25 M sucrose, 5 mM Tris–HCl, pH 7.5, and 0.1 mM PMSF) and homogenized using a glass–Teflon homogenizer. Unbroken cells and nuclei were pelletted by centrifugation at 600*g* for 15 min. Supernatants were centrifuged at 10 000*g* for 25 min, and the mitochondrial pellet was washed once with the isotonic buffer containing 1 mM EDTA, pH 8.

Western blot analysis

COS-7 and HeLa cells were seeded in 100-mm diameter dishes and grown to 70–80% conlluency. Cells were

transfected with a complex consisting of 7 μg of plasmid DNA and 21 μl of the liposomal transfection reagent Metafectene (Biontex Laboratories GmbH, Munich, Germany) in 4 ml of OptiMem (Invitrogen) according to the manufacturer's instructions. After 5 h, 4 ml of DMEM 20% FBS was added; the medium was replaced after 12 h and cells were collected after 24 h for western blot.

Proteins were quantified by using the Bio-Rad Protein Assay (Bio-Rad, Hercules, CA, USA); samples (50 μg) were subjected to SDS–PAGE on a 12% gel and were transferred to Hybond C (Amersham Biosciences AB Biosciences AB) by standard western blotting techniques. Blots were incubated with the relevant primary antisera at dilutions recommended by the manufacturers. After washing in PBS containing 0.05% Tween-20, blots were incubated with relevant HRP-conjugated secondary antisera and developed using a chemiluminescence detection kit (Amersham Biosciences AB Pharmacia Biotech).

Immunofluorescence analysis

HeLa and COS-7 cells were grown for 16 h prior to transfection on glass cover slips in 12-well plates. Transfections were carried out using 300 ng of plasmid DNA for 10^5 cells and 3 μl of the liposomal transfection reagent Metafectene (Biontex Laboratories) in 1 ml of OptiMem according to the manufacturer's instructions. After 5 h, 1 ml of DMEM 20% FBS was added; the medium was replaced after 12 h. After 24 h, cells were washed with PBS and fixed in 4% paraformaldehyde/PBS for 30 min at ambient temperature. After three PBS washes, cells were permeabilized by incubation in PBS containing 0.2% Triton-X100 and 10% donkey serum for 1 h. The cells were incubated for 2 h at room temperature with primary antibodies resuspended in PBS plus 0.1% Triton-X100 and 1% donkey serum: mouse monoclonal anti-HA antibodies (1 : 500 dilution; BAbCO, Richmond, CA); goat polyclonal anti-c-Myc antibodies (1 : 200 dilution, NOVUS Biologicals, Littleton, CO); rabbit polyclonal anti-AFG3L2 antibodies (1 : 200 dilution); rabbit polyclonal anti-calnexin antibodies (1 : 500 dilution; Sigma, St Louis, MO); mouse monoclonal anti-LAMP1 (1 : 100 dilution; Developmental Studies Hybridoma Bank, IA); rabbit polyclonal anti-GFP (1 : 500 dilution; Molecular Probes, Eugene, OR); mouse monoclonal anti-TOM20 (1 : 500; Molecular Probes). After PBS washing, primary antibodies were visualized using the appropriate donkey anti-mouse, or donkey anti-rabbit antibodies conjugated with either Alexa Fluor 488 or Alexa Fluor 594 (Molecular Probes). After PBS washes, cells were mounted on glass slides using Dako Mounting Medium (Dako, Carpinteria, CA) and visualized under confocal microscope BioRad Leica TCS SP2 AOBS (Leica Microsystems, Bannockburn, IL). Overlap coefficient (R) values were calculated using the ImageProPlus software (Media Cybernetics, Silver Spring, MD, USA).

Immunogold labeling and electron microscopy

HeLa cells were cultured in 10-cm tissue culture dishes and transfected with the wild-type and mutant PINK1 proteins using the Metafectene transfection reagent, according to the manufacturer's protocol. After 24 h, cells were fixed with the aldehyde mixture, then detached and recovered by centrifugation. After extensive washes with phosphate buffer, the pellets were dehydrated in ethanol and embedded in LR White (42). Ultrathin sections were collected over nicked grids, exposed for 90 min at 37°C to the mouse anti-HA Ab diluted in phosphate–glycine buffer, and then labeled with anti-IgG-coated gold particles (12 nm). After washing, the grids were post-fixed with 1% glutaraldehyde in phosphate buffer and then stained with uranyl acetate and lead citrate. Samples were examined in a LEO 912AB transmission electron microscope.

Integral membrane protein solubility assay

Detergent-soluble and -insoluble fractions were prepared from 100 μg of mitochondrial proteins, isolated from transfected HeLa cells, by homogenization in TNE buffer (10 mM Tris–HCl, pH 7.4; 150 mM NaCl; 1 mM EDTA, pH 8), containing protease inhibitor cocktail (Sigma) and different detergents: non-ionic detergent Triton X-100 (0.1, 0.5, 2 and 5%); non-denaturing zwitterionic detergent CHAPS (0.1, 0.5, 2 and 5%), surfactant-like detergent digitonin (0.1, 0.5, 2 and 5%) and anionic detergent Sarkosyl (0.1, 0.5, 2 and 5%). After incubation of mitochondria at 4°C for 20 min in agitation, the homogenates were centrifuged (20 min at 13 000g) and the resulting pellet (detergent-insoluble) and supernatant (detergent-soluble) fractions were collected and analyzed by western blotting.

In vitro import assay

Mitochondria from HeLa cells were isolated as described previously, and import assay was performed (43). Precursor proteins PINK1 wt, $PINK1^{W437X}$, $PINK1^{G309D}$ and $PINK1^{A168P}$ were synthesized by *in vitro* transcription and translation in the presence of [^{35}S]methionine (TNT-coupled reticulocyte lysate system; Promega). The mitochondrial import assay was performed as follows, in the presence or in the absence of valinomycin: 1 mg of mitochondria was resuspended in 35 μl of mannitol buffer (225 mM mannitol, 25 mM sucrose, 10 mM Tris–HCl, pH 7.8, and 0.1 mM EDTA) and incubated with 70 μl of reticulocyte lysate-synthesized PINK1, 0.6 μl of 180 mM malate, and 1.1 μl of 1 M pyruvate. After 10 min of incubation at room temperature, samples were transferred at 37°C and 20 μl aliquots were removed at 0, 15 and 45 min, transferred to a fresh tube and centrifuged at 10 000g for 5 min. When indicated, mitochondria were treated with proteinase K (0.5 μg/mg mitochondria) for 10 min on ice. Pellets were washed two times with mannitol buffer and resuspended in sample buffer for electrophoretic analysis in 10% SDS–PAGE. The imported protein was analyzed by autoradiography.

Protease protection assay

Protease protection experiments were done as described by Griparic *et al*. (44). Briefly, 0.5 mg mitochondria from PINK1 wt and $PINK1^{W437X}$ transfected cells were resuspended in isolation buffer (70 mM sucrose, 220 mM mannitol,

2 mM HEPES, 0.5 mg/ml bovine serum albumin). Trypsin (0, 10, 25 and 100 μg/ml) and digitonin (2.5 mg/mg mitochondria) were added. After 30 min of incubation on ice, the reaction was stopped by adding trichloroacetic acid (TCA). The protein pellets were resuspended in SDS sample buffer and electrophoretically analyzed by SDS–PAGE.

Autophosphorylation assay

For the autophosphorylation assay, 10 pmol of GST-fused PINK1 proteins were incubated at 30°C for 45 min in 20 μl of a buffer consisting of 20% glycerol, 10 mM $MgCl_2$, 3 mM $MnCl_2$, 1 mM DTT, 40 mM HEPES (pH 7.4), protease inhibitor cocktail (Sigma), 100 μM ATP and 6 μCi [γ-^{32}P]ATP. The reaction was stopped by addition of SDS-sample buffer. Phosphorylated proteins were separated on a 10% SDS–polyacrylamide gel and transferred to Hybond C (Amersham Biosciences AB Pharmacia Biotech) by standard western blotting technique. Membranes were exposed to X-ray film at −80°C.

Substrate-phosphorylation assay

Substrate phosphorylation by GST-PINK1 proteins was performed in a 20 μl reaction buffer containing 20% glycerol, 10 mM $MgCl_2$, 3 mM $MnCl_2$, 1 mM DTT, 40 mM HEPES (pH 7.4), protease inhibitor cocktail (Sigma), 100 μM ATP and 6 μCi [γ-^{32}P]ATP, 10 pmol of GST-Pink1 proteins and 10 pmol of the dephosphorylated form of α-casein (Sigma) at 30°C for 45 min. The reaction was initiated by the addition of 10 pmol of PINK1 proteins and terminated by adding SDS sample buffer. Phosphorylated proteins were separated on a 12% SDS–polyacrylamide gel and transferred to Hybond C (Amersham Biosciences AB Pharmacia Biotech) by standard western blotting technique. Membranes were exposed to X-ray film at −80°C.

Protein modeling

For the analysis of PINK1 structure, we used the homology model from ModBase (residues 151–501 modeled on the PDB structure 1gjo as template). As starting structure for MD simulations, the PINK1 model was used for the wild-type study and after mutation of the side chain of residue 168 from alanine to proline for the mutant study. Cysteines were assumed to be in the reduced state. A water sphere (40 Å radius) was built around the proteins, the system was minimized for 500 steps (2 fs per step) and the MD was subsequently carried out for 25 000 steps (50 ps) at a temperature of 310 K under periodic boundary conditions. The program NAMD (v2.5) with the CHARMM 27 parameter set was used for MD simulations. The volumes of the ATP/ADP binding pockets have been obtained from castP analysis using the protein atomic coordinates obtained from the MD at the specified times of simulation.

The model of a PINK1/substrate complex was built according to the experimental topology of the complex formed by the cAMP-dependent protein kinase and a 20-residue substrate (pdb 1JBP). The ATP ligand was positioned onto PINK1 according to the geometry found in the pdb structure 1H1W, which contains a kinase/ATP complex.

ACKNOWLEDGEMENTS

We thank Cesare Covino and Maria Carla Panzeri from the Advanced Light and Electron Microscopy BioImaging Center (Alembic) at the Università Vita e Salute San Raffaele for their contribution to confocal analysis and immunogold staining. We gratefully acknowledge the support of the Italian Telethon Foundation (grant no. GGP04291), the Italian Ministry of Health (Ricerca Finalizzata 2003) and MIUR (FIRB grant no. RBNE01JJ45). "Funding to pay the Open Access publication charges for this article was provided by the Italian Telethon Foundation".

Conflict of Interest statement. None declared.

REFERENCES

1. Dauer, W. and Przedborski, S. (2003) Parkinson's disease: mechanisms and models. *Neuron*, **39**, 889–909.
2. Vila, M. and Przedborski, S. (2004) Genetic clues to the pathogenesis of Parkinson's disease. *Nat Med*., **10** (suppl.), S58–S62.
3. Valente, E.M., Abou-Sleiman, P.M., Caputo, V., Muqit, M.M., Harvey, K., Gispert, S., Ali, Z., Del Turco, D., Bentivoglio, A.R., Healy, D.G. *et al*. (2004) Hereditary early-onset Parkinson's disease caused by mutations in PINK1. *Science*, **304**, 1158–1160.
4. Valente, E.M., Salvi, S., Ialongo, T., Marongiu, R., Elia, A.E., Caputo, V., Romito, L., Albanese, A., Dallapiccola, B. and Bentivoglio, A.R. (2004) PINK1 mutations are associated with sporadic early-onset parkinsonism. *Ann. Neurol*. **56**, 336–341.
5. Hatano, Y., Li, Y., Sato, K., Asakawa, S., Yamamura, Y., Tomiyama, H., Yoshino, H., Asahina, M., Kobayashi, S., Hassin-Baer, S. *et al*. (2004) Novel PINK1 mutations in early-onset parkinsonism. *Ann. Neurol*., **56**, 424–427.
6. Rohe, C.F., Montagna, P., Breedveld, G., Cortelli, P., Oostra, B.A. and Bonifati, V. (2004) Homozygous PINK1 C-terminus mutation causing early-onset parkinsonism. *Ann. Neurol*., **56**, 427–431.
7. Unoki, M. and Nakamura, Y. (2001) Growth-suppressive effects of BPOZ and EGR2, two genes involved in the PTEN signaling pathway. *Oncogene*, **20**, 4457–4465.
8. Nakajima, A., Kataoka, K., Hong, M., Sakaguchi, M. and Huh, N.H. (2003) BRPK, a novel protein kinase showing increased expression in mouse cancer cell lines with higher metastatic potential. *Cancer Lett*., **201**, 195–201.
9. Manning, G., Whyte, D.B., Martinez, R., Hunter, T. and Sudarsanam, S. (2002) The protein kinase complement of the human genome. *Science*, **298**, 1912–1934.
10. Yamamoto, A., Friedlein, A., Imai, Y., Takahashi, R., Kahle, P.J. and Haass, C. (2005) Parkin phosphorylation and modulation of its E3 ubiquitin ligase activity. *J. Biol Chem*., **280**, 3390–3399.
11. Fujiwara, H., Hasegawa, M., Dohmae, N., Kawashima, A., Masliah, E., Goldberg, M.S., Shen, J., Takio, K. and Iwatsubo, T. (2002) alpha-Synuclein is phosphorylated in synucleinopathy lesions. *Nat. Cell Biol*. **4**, 160–164.
12. Chen, L. and Feany, M.B. (2005) Alpha-synuclein phosphorylation controls neurotoxicity and inclusion formation in a *Drosophila* model of Parkinson disease. *Nat. Neurosci*., **8**, 657–663.
13. Paisan-Ruiz, C., Jain, S., Evans, E.W., Gilks, W.P., Simon, J., van der Brug, M., de Munain, A.L., Aparicio, S., Gil, A.M., Khan, N. *et al*. (2004) Cloning of the gene containing mutations that cause PARK8-linked Parkinson's disease. *Neuron*, **44**, 595–600.
14. Zimprich, A., Biskup, S., Leitner, P., Lichtner, P., Farrer, M., Lincoln, S., Kachergus, J., Hulihan, M., Uitti, R.J., Calne, D.B. *et al*. (2004) Mutations in LRRK2 cause autosomal-dominant parkinsonism with pleomorphic pathology. *Neuron*, **44**, 601–607.
15. Cookson, M.R. (2003) Pathways to Parkinsonism. *Neuron*, **37**, 7–10.
16. Trojanowski, J.Q. (2003) Rotenone neurotoxicity: a new window on environmental causes of Parkinson's disease and related brain amyloidoses. *Exp. Neurol*., **179**, 6–8.

17. Jenner, P. (1998) Oxidative mechanisms in nigral cell death in Parkinson's disease. *Mov Disord*. **13** (Suppl. 1), 24–34.
18. Hsu, L.J., Sagara, Y., Arroyo, A., Rockenstein, E., Sisk, A., Mallory, M., Wong, J., Takenouchi, T., Hashimoto, M. and Masliah, E. (2000) Alpha-Synuclein promotes mitochondrial deficit and oxidative stress. *Am. J. Pathol*., **157**, 401–410.
19. Tanaka, Y., Engelender, S., Igarashi, S., Rao, R.K., Wanner, T., Tanzi, R.E., Sawa, A., Dawson, V.L., Dawson, T.M. and Ross, C.A. (2001) Inducible expression of mutant alpha-synuclein decreases proteasome activity and increases sensitivity to mitochondria-dependent apoptosis. *Hum. Mol. Genet*., **10**, 919–926.
20. Sherer, T.B., Betarbet, R., Stout, A.K., Lund, S., Baptista, M., Panov, A.V., Cookson, M.R. and Greenamyre, J.T. (2002) An *in vitro* model of Parkinson's disease: linking mitochondrial impairment to altered alpha-synuclein metabolism and oxidative damage. *J. Neurosci*., **22**, 7006–7015.
21. Sherer, T.B., Betarbet, R., Testa, C.M., Seo, B.B., Richardson, J.R., Kim, J.H., Miller, G.W., Yagi, T., Matsuno-Yagi, A. and Greenamyre, J.T. (2003) Mechanism of toxicity in rotenone models of Parkinson's disease. *J. Neurosci*., **23**, 10756–10764.
22. Canet-Aviles, R.M., Wilson, M.A., Miller, D.W., Ahmad, R., McLendon, C., Bandyopadhyay, S., Baptista, M.J., Ringe, D., Petsko, G.A. and Cookson, M.R. (2004) The Parkinson's disease protein DJ-1 is neuroprotective due to cysteine-sulfinic acid-driven mitochondrial localization. *Proc. Natl Acad. Sci. USA*, **101**, 9103–9108.
23. Claros, M.G. and Vincens, P. (1996) Computational method to predict mitochondrially imported proteins and their targeting sequences. *Eur. J. Biochem*., **241**, 779–786.
24. Cserzo, M., Wallin, E., Simon, I., von Heijne, G. and Elofsson, A. (1997) Prediction of transmembrane alpha-helices in prokaryotic membrane proteins: the dense alignment surface method. *Protein Eng*., **10**, 673–676.
25. Atorino, L., Silvestri, L., Koppen, M., Cassina, L., Ballabio, A., Marconi, R., Langer, T. and Casari, G. (2003) Loss of m-AAA protease in mitochondria causes complex I deficiency and increased sensitivity to oxidative stress in hereditary spastic paraplegia. *J. Cell Biol*., **163**, 777–787.
26. Kyte, J. and Doolittle, R.F. (1982) A simple method for displaying the hydropathic character of a protein. *J. Mol. Biol*., **157**, 105–132.
27. Casari, G., De Fusco, M., Ciarmatori, S., Zeviani, M., Mora, M., Fernandez P., De Michele, G., Filla, A., Cocozza, S., Marconi, R. *et al*. (1998) Spastic paraplegia and OXPHOS impairment caused by mutations in paraplegin, a nuclear-encoded mitochondrial metalloprotease. *Cell*, **93**, 973–983.
28. Schapira, A.H. (2002) Primary and secondary defects of the mitochondrial respiratory chain. *J. Inherit. Metab. Dis*., **25**, 207–214.
29. Rothbauer, U., Hofmann, S., Muhlenbein, N., Paschen, S.A., Gerbitz, K.D., Neupert, W., Brunner, M. and Bauer, M.F. (2001) Role of the deafness dystonia peptide 1 (DDP1) in import of human Tim23 into the inner membrane of mitochondria. *J. Biol. Chem*., **276**, 37327–37334.
30. Panov, A.V., Gutekunst, C.A., Leavitt, B.R., Hayden, M.R., Burke, J.R., Strittmatter, W.J. and Greenamyre, J.T. (2002) Early mitochondrial calcium defects in Huntington's disease are a direct effect of polyglutamines. *Nat. Neurosci*., **5**, 731–736.
31. Beilina, A., Van Der Brug, M., Ahmad, R., Kesavapany, S., Miller, D.W., Petsko, G.A. and Cookson, M.R. (2005) Mutations in PTEN-induced putative kinase 1 associated with recessive parkinsonism have differential effects on protein stability. *Proc. Natl Acad. Sci. USA*, **102**, 5703–5708.
32. Da Cruz, S., Xenarios, I., Langridge, J., Vilbois, F., Parone, P.A. and Martinou, J.C. (2003) Proteomic analysis of the mouse liver mitochondrial inner membrane. *J. Biol. Chem*., **278**, 41566–41571.
33. Garofalo, T., Giammarioli, A.M., Misasi, R., Tinari, A., Manganelli, V., Gambardella, L., Pavan, A., Malorni, W. and Sorice, M. (2005) Lipid microdomains contribute to apoptosis-associated modifications of mitochondria in T cells. *Cell Death Differ*, **12**, 1378–1389.
34. Huse, M. and Kuriyan, J. (2002) The conformational plasticity of protein kinases. *Cell*, **109**, 275–282.
35. Horbinski, C. and Chu, C.T. (2005) Kinase signaling cascades in the mitochondrion: a matter of life or death. *Free Radic. Biol. Med*., **38**, 2–11.
36. Technikova-Dobrova, Z., Sardanelli, A.M., Speranza, F., Scacco, S., Signorile, A., Lorusso, V. and Papa, S. (2001) Cyclic adenosine monophosphate-dependent phosphorylation of mammalian mitochondrial proteins: enzyme and substrate characterization and functional role. *Biochemistry*, **40**, 13941–13947.
37. Murriel, C.L., Churchill, E., Inagaki, K., Szweda, L.I. and Mochly-Rosen, D. (2004) Protein kinase Cdelta activation induces apoptosis in response to cardiac ischemia and reperfusion damage: a mechanism involving BAD and the mitochondria. *J. Biol. Chem*., **279**, 47985–47991.
38. Seutin, V., Shen, K.Z., North, R.A. and Johnson, S.W. (1996) Sulfonylurea-sensitive potassium current evoked by sodium-loading in rat midbrain dopamine neurons. *Neuroscience*, **71**, 709–719.
39. Mazzio, E.A., Reams, R.R. and Soliman, K.F. (2004) The role of oxidative stress, impaired glycolysis and mitochondrial respiratory redox failure in the cytotoxic effects of 6-hydroxydopamine *in vitro*. *Brain Res*., **1004**, 29–44.
40. Riedl, S.J. and Shi, Y. (2004) Molecular mechanisms of caspase regulation during apoptosis. *Nat. Rev. Mol. Cell Biol*., **5**, 897–907.
41. Smith, A.L. (1967) Preparation, properties and conditions for assay of mitochondria: slaughterhouse material, small-scale. *Meth. Enzymol*., **10**, 81–86.
42. Newman, J. and Antonakopoulos, G.N. (1989) The fine structure of the human fetal urinary bladder: development and maturation. A light, transmission and scanning electron microscopic study. *J. Anat*., **166**, 135–150.
43. Yano, M., Hoogenraad, N., Terada, K. and Mori, M. (2000) Identification and functional analysis of human Tom22 for protein import into mitochondria. *Mol. Cell Biol*., **20**, 7205–7213.
44. Griparic, L., van der Wel, N.N., Orozco, I.J., Peters, P.J. and van der Bliek, A.M. (2004) Loss of the intermembrane space protein Mgm1/OPA1 induces swelling and localized constrictions along the lengths of mitochondria. *J. Biol. Chem*., **279**, 18792–18798.